

Locating influential nodes in hypergraphs via fuzzy collective influence

Su-Su Zhang^a, Xiaoyan Yu^a, Gui-Quan Sun^{b,c,*}, Chuang Liu^{a,*}, Xiu-Xiu Zhan^{a,d,*},

^a*Research Center for Complexity Sciences, Hangzhou Normal University, Hangzhou 311121, PR China*

^b*Sino-Europe Complex Science Center, School of Mathematics, North University of China, Shanxi, Taiyuan 030051, China*

^c*Complex Systems Research Center, Shanxi University, Shanxi, Taiyuan 030006, China*

^d*College of Media and International Culture, Zhejiang University, Hangzhou 310058, PR China*

Abstract

Complex contagion phenomena, such as the spread of information or contagious diseases, often occur among the population due to higher-order interactions between individuals. Individuals who can be represented by nodes in a network may play different roles in the spreading process, and thus finding the most influential nodes in a network has become a crucial topic in network science for applications such as viral marketing, rumor suppression, and disease control. To solve the problem of identifying nodes that have high influence in a complex system, we propose a higher-order distance-based fuzzy centrality methods (HDF and EHDF) that are customized for a hypergraph which can characterize higher-order interactions between nodes via hyperedges. The methods we proposed assume that the influence of a node is reliant on the neighboring nodes with a certain higher-order distance. We compare the proposed methods with the baseline centrality methods to verify their effectiveness. Experimental results on six empirical hypergraphs show that the proposed methods could better identify influential nodes, especially showing plausible performance in finding the top influential nodes. Our proposed theoretical framework for iden-

*Corresponding authors.

Email addresses: gquansun@126.com (Gui-Quan Sun), liuchuang@hznu.edu.cn (Chuang Liu), zhanxiuxiu@hznu.edu.cn (Xiu-Xiu Zhan)

tifying influential nodes could provide insights into how higher-order topological structure can be used for tasks such as vital node identification, influence maximization, and network dismantling.

Keywords: Hypergraph, Influential Node, SIR Model, Fuzzy Collective Influence

1. Introduction

Recently, research on measuring the influence of the nodes in a network is of theoretical and practical significance [5, 8], given that it has the potential to be utilized in various contexts including disease control [3, 20], drug targeting [11, 13], information dissemination [12, 15] and network security [16, 21]. Classical influential node identification methods primarily concentrate on simple networks, which refer to networks composed of pairwise interactions between nodes [2, 6, 9, 29]. However, a growing body of evidence indicates that real-world complex systems involve interactions among entities that go beyond simple pairwise relationships. A case in point is that users may form groups on social platforms to exchange emotions and ideas. Besides, multiple researchers may work together on the same project and a single drug may impact more than two proteins. The multiple interactions between entities in a complex system are usually represented by hyperedges in a hypergraph or simplicial complex [31, 33]. And in this work, we aim to characterize influential nodes on a hypergraph.

Previous researchers have conducted preliminary investigations on the identification of influential nodes in hypergraphs [18, 30]. Methods that consider the local or global topological structure of a hypergraph have been proposed. For example, degree [22, 26], hyperdegree [4], and hyperedge degree are methods based on the local neighbors of a node or a hyperedge. Meanwhile, vector centrality [17], eccentricity centrality, and harmonic closeness centrality are methods based on the global structure of a hypergraph that were originally designed to evaluate the importance of a hyperedge. Recently, some work has started exploring the use of higher-order distances for the identification of important

nodes, such as s -eccentricity centrality, s -harmonic closeness centrality [1], and gravity-based centrality [10, 19, 27, 32, 35]. While the methods mentioned above have demonstrated their efficacy in identifying essential nodes in terms of network connectivity, they have certain limitations when it comes to identifying influential nodes.

To fill this gap, we propose a higher-order distance-based fuzzy centrality to find the most influential nodes in a hypergraph. To quantify the influence of a target node, we assume that nodes that are surrounded by influential nodes are more influential. Therefore, we use a ball that is centered at the target node and with a radius determined by a higher-order distance to determine the number of surrounding nodes of the target node. Furthermore, the influence of the target nodes is computed by collecting the influence of nodes inside the ball using fuzzy sets [23, 34] and Shannon entropy [25]. Experimental results demonstrate that the method we proposed can accurately identify influential nodes compared to state-of-the-art baselines.

The rest of this paper is structured as follows: in Section 2, we provide the definition of a hypergraph and the higher-order distance on a hypergraph. In Section 3, we provide a comprehensive explanation of the intricate steps involved in the higher-order distance-based fuzzy centrality. Additionally, we demonstrate the use of an SIR model to accurately represent the actual influence of a node. In Section 4, we present the baselines and provide an overview of the datasets. Furthermore, the effectiveness of the proposed method is tested in Section 5. We highlight the theoretical and practical implications to conclude the paper in Section 6 and Section 7.

2. Preliminary definition

2.1. Definition of a hypergraph

An unweighted and undirected hypergraph $H = (V, E)$ contains a node set $V = \{v_1, v_2, v_3, \dots, v_N\}$ and a hyperedge set $E = \{e_1, e_2, e_3, \dots, e_M\}$, where a hyperedge implies interactions between multiple nodes. We construct an in-

incidence matrix I to represent the relationship between nodes and hyperedges, i.e., if node v_i belongs to a hyperedge e_j , then $I_{ij} = 1$; otherwise, it is set to 0. Mathematically speaking, it can be expressed as follows:

$$I_{ij} = \begin{cases} 1 & \text{if node } v_i \text{ belongs to hyperedge } e_j, \\ 0 & \text{otherwise.} \end{cases} \quad (1)$$

Accordingly, the adjacency matrices A of H is obtained via the incidence matrix I , i.e.,

$$A_{ij} = [II^T - D]_{ij}, \quad (2)$$

where D is the diagonal matrix, D_{ii} represents the number of hyperedges that node v_i belongs to, and A_{ij} stands for the number of hyperedges which contain both node v_i and v_j . We show an example of a hypergraph with 11 nodes and 4 hyperedges in Figure 1(a), where its incidence and adjacency matrix are given in Figure 1(b) and (c).

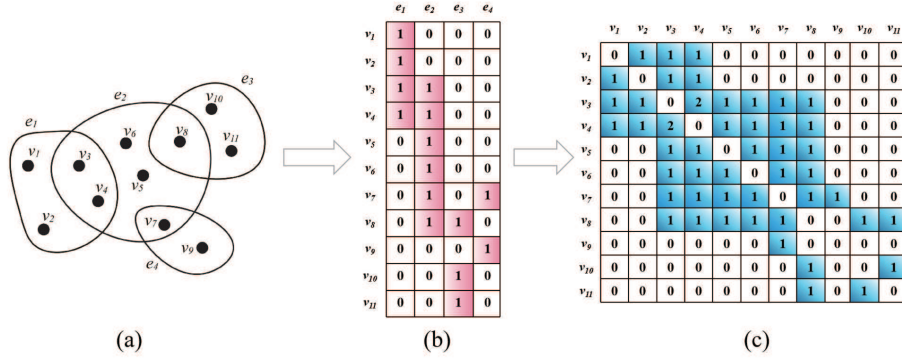


Figure 1: An illustrative example of a hypergraph: (a) a hypergraph with 11 nodes and 4 hyperedges; (b) the incidence matrix of the hypergraph given in (a); (c) the adjacency matrix of the hypergraph given in (a).

2.2. Definition of higher-order distance

In a hypergraph, two hyperedges are s adjacent if they share at least s common nodes. An s -walk w_i^l with a length equal to l is a sequence of nodes [1]

which is expressed as follows:

$$w_i^l = e_{i_0}, e_{i_1}, e_{i_2}, \dots, e_{i_{l-1}}, e_{i_l}; \quad (3)$$

where $|e_{i_{j-1}} \cap e_{i_j}| \geq s$, $j = 1, \dots, l$, $s \geq 1$. Thus, an s -path between two hyperedges is an s -walk with nonrepeated nodes, and the s -distance $d_s^e(p, q)$ between hyperedges e_p and e_q is given by the length of the shortest s -path between them. In particular, the distance is ∞ if there is no s -path between two hyperedges.

We define the distance between two nodes on the basis of the distance between two hyperedges. Suppose that nodes v_i and v_j belong to hyperedges e_p and e_q , the s -distance between v_i and v_j is denoted as $d_s^v(i, j)$ and can be mathematically expressed as:

$$d_s^v(i, j) = \begin{cases} 1 & \text{if } e_p = e_q \\ d_s^e(p, q) + 1 & \text{otherwise.} \end{cases} \quad (4)$$

3. Method

In this section, we will first introduce the proposed method, higher-order distance-based fuzzy centrality, for the assessment of influential nodes. The proposed method is based on the assumption that a node's influence is based on the collective influence of its higher-order neighbors, and we utilize the fuzzy sets and Shannon entropy to define the proposed centrality. Later on, we propose to use the SIR model in a hypergraph to quantify a node's real spread ability, which will be used to evaluate the effectiveness of our method.

3.1. Higher-order distance-based fuzzy centrality

For a central node v_i , we assume that the nodes close to it can influence it more. Therefore, we use fuzzy sets to define the influence of a node that is at s -distance l_i^s on v_i as

$$X(l_i^s) = \exp\left(-\frac{(l_i^s)^2}{(L_i^s)^2}\right), \quad (5)$$

where l_i^s represents the s -distance from the center node v_i , and L_i^s is the radius of the $Ball(i, L_i^s)$ we consider and is given by

$$L_i^s = \lceil \frac{z_i^s}{r} \rceil, \quad (6)$$

where z_i^s is the maximum s -distance from node v_i to other nodes and r is a tunable parameter. By adjusting r , we can determine the number of nodes inside $Ball(i, L_i^s)$ that will influence v_i , i.e., with a smaller value of r indicating a larger radius and thus more nodes will be incorporated into the ball. The notation $\lceil \cdot \rceil$ means we round the value up. By using the fuzzy sets, a node that is at s -distance l_i^s to v_i has $X(l_i^s)$ influence on v_i , and we have $\frac{1}{e} \leq X(l_i^s) < 1$. When the value of $X(l_i^s)$ tends to 1, it indicates that nodes located at a distance of l_i^s from v_i have a greater impact on its influence.

Furthermore, we assume that the number of nodes with the distance of l_i^s from node v_i is denoted as $n(l_i^s)$. The fuzzy number of nodes at distance l_i^s to the node v_i is represented as

$$f(l_i^s) = n(l_i^s)X(l_i^s) \quad (7)$$

Thus, we use $F(L_i^s) = \sum_{l_i^s=1}^{L_i^s} f(l_i^s)$ to represent the fuzzy number of nodes in $Ball(i, L_i^s)$. And $p(l_i^s)$ denotes the fraction of nodes whose shortest s -distance from node v_i is l_i^s , which is given by

$$p(l_i^s) = \frac{1}{e} \frac{f(l_i^s)}{F(L_i^s)}, \quad (8)$$

in the above equation, we use $\frac{1}{e}$ as a scaling factor to refine the probabilities to the range of $[0, \frac{1}{e}]$ in order to use Shannon entropy for node influence characterization.

We use the above fuzzy sets and probability to measure the influence of node

v_i , the equation is given as follows:

$$C_{HDF}(i) = \frac{\sum_{s=1}^{s_m} C_{HDF}^s(i)}{s_m}, \quad (9)$$

where $C_{HDF}^s(i) = \sum_{l_i^s=1}^{L_i^s} \frac{-p(l_i^s) \ln(p(l_i^s))}{(l_i^s)^2}$ is the s -distance fuzzy centrality of node v_i , and $s_m (1 \leq s_m \leq s_M)$ a tunable parameter. The equation shows that we comprehensively consider the local fuzzy centrality with different s -distance to measure the influence of a node.

For clarity, we give a toy example of how to compute the influence of a node based on HDF, which is shown in Figure 2. In the figure, we set v_5 as the target node, and $r = 1$, $s_m = 2$. Figure 2(a) and (b) show the calculation of 1-distance and 2-distance fuzzy centrality for node v_5 , and the values of them are $C_{HDF}^1(v_5) = 0.4096$ and $C_{HDF}^2(v_5) = 0.4045$, respectively. Therefore, the final HDF centrality for node v_5 which considers the information of different s -distances can be calculated as:

$$C_{HDF}(v_5) = \frac{\sum_{s=1}^2 C_{HDF}^s(v_5)}{2} = \frac{C_{HDF}^1(v_5) + C_{HDF}^2(v_5)}{2} = 0.8141 \quad (10)$$

In HDF, we use the maximum s -distance from v_i to other nodes, i.e., z_i^s , to determine the radius of the $Ball(i, L_i^s)$. We further incorporate all the s -distances when determining the radius, i.e., we define $L_i^{es} = \lceil \frac{\sum_{s=1}^{s_m} z_i^s}{s_m * r} \rceil$. The other procedures are the same as HDF, and we call the new centrality method using L_i^{es} as the radius as EHDF, that is, extended higher-order distance-based fuzzy centrality.

3.2. SIR spreading model on a hypergraph

We extend a Susceptible-Infected-Recovered (SIR) model to mimic the spreading process in a hypergraph. In the process of spreading, the nodes may be in one of the three states: Susceptible (S), Infected (I), and Recovered (R). When a node v_i is infected, it will turn to the state I and can randomly infect nodes that are in the same hyperedge. Every infected node has a chance of recovering

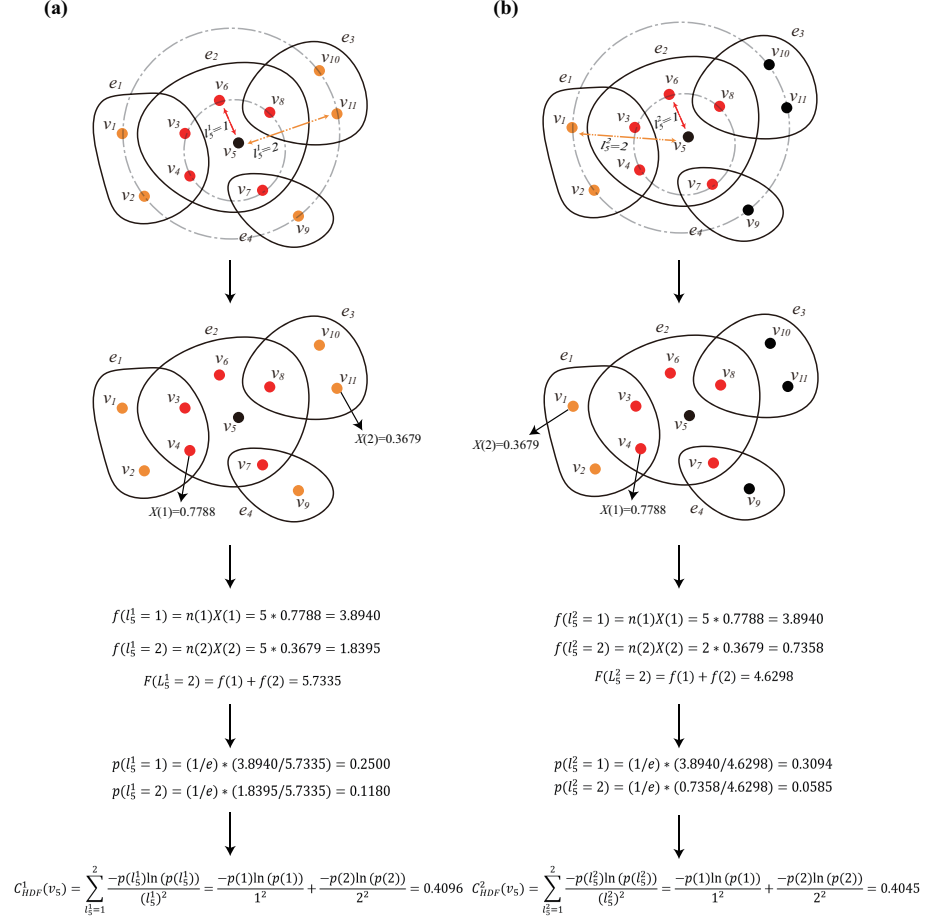


Figure 2: A toy example of calculating higher-order distance-based fuzzy centrality. The target node is v_5 and $r = 1$, $s_m = 2$. The red and orange nodes represent the first and second order of neighboring nodes of v_5 , respectively. We show the calculation of (a) 1-distance fuzzy centrality for node v_5 ; (b) 2-distance fuzzy centrality for node v_5 .

to the state R independently with a probability of μ . Once a node is in the R state, it cannot be infected by any other nodes. We note that we use E_i to denote the set of hyperedges to which node v_i belongs. Details of the SIR model in the hypergraph are given below.

- Initially, the seed node is labeled as the I state, while the rest nodes are in the S state. It is noted that no nodes are in the R state at the beginning.
- In time step t , a hyperedge e_j will be selected uniformly at random from

E_i for each infected node v_i . And for every S -state node belonging to e_j , it will be infected by node v_i with probability β . At the same time, the nodes in the I state have a probability μ to recover to the R state.

- The contagion process continues until the time step T .

We use the number of infected and recovered at the time step T to quantify the spread capacity of the selected seed node, where T is a tunable parameter. Furthermore, we set the infection probability β slightly higher than the spreading threshold β_0 to ensure that the spreading model can spread out on a hypergraph.

We present a visual spread process of the SIR model on a hypergraph in Figure 3. At the initial time step $t = 0$, node v_7 is assigned as the seed in I state. The set of hyperedges that contains node v_7 is $E_7 = \{e_2, e_4\}$. In time step $t = 1$, hyperedge e_2 is randomly selected and nodes v_3, v_8 are infected by node v_7 , and no nodes are recovered in this step. Subsequently, infection occurs in hyperedge e_1 and e_3 at time step $t = 2$, with nodes v_2, v_4 and v_{11} infected and v_7 recovered.

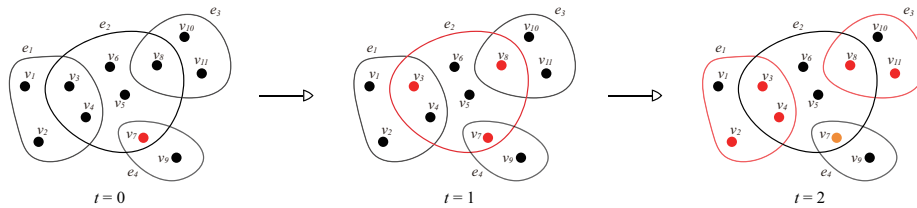


Figure 3: An example of the SIR model on a hypergraph. The black, red, and orange nodes correspond to the S , I , and R nodes, respectively. The red hyperedge indicates that the spread is happening on it.

4. Baselines and Datasets

To validate the effectiveness of the proposed methods, we introduce the state-of-the-art methods, including the family of degree centralities and centrality based on higher-order structures, as baselines. Moreover, the datasets for constructing empirical hypergraphs will be illustrated in this section as well.

4.1. Baselines

Degree Centrality (DC) measures the importance of a node by quantifying the number of neighbors, and thus the degree of node v_i is given by

$$k_i = \sum_{j=1}^N A_{ij}, \quad (11)$$

where A is the adjacency matrix and N is the number of nodes of the hypergraph.

Hyper Degree Centrality (HDC) assumes that if a node belongs to more hyperedges, it has a greater chance of spreading the influence widely. The HDC of a node v_i reads as

$$k_i^H = \sum_{m=1}^M I_{im}, \quad (12)$$

where I is the incidence matrix, and M is the number of hyperedges.

Vector Centrality (VC) evaluates the centrality of nodes by first characterizing the centrality of the hyperedges[17]. Specifically, we first project the hypergraph into a line graph¹, and then calculate the eigenvector centrality values of all hyperedges. Then, the centrality value of the hyperedge will be evenly distributed to each node within the hyperedge. For a node v_i , suppose that the hyperedges containing v_i are given by the set $E_i = \{e_{i1}, e_{i2}, \dots, e_{iK}\}$, which will be used in the definition of the following centrality measures. We use c_i to represent the vector centrality of v_i , which is given by

$$c_i = \sum_{k=1}^K c_{ik}, \quad (13)$$

where c_{ik} is the centrality value distributed from hyperedge e_{ik} .

Hyperedge Degree Centrality (HEDC): Given the line graph of a hy-

¹The line graph $L(H)$ is a graph of M nodes. The nodes and hyperedges in $H(V, E)$ are mapped to edges and nodes in $L(H)$, respectively. That is to say, if two hyperedges e_p and e_q share at least one common node, there is an edge between node v_p and v_q in the line graph $L(H)$.

pergraph, we use matrix \mathcal{A} to represent the adjacent relationship between two hyperedges, with $\mathcal{A}_{ij} = 1$ meaning that the hyperedges e_i and e_j share at least one node and otherwise $\mathcal{A}_{ij} = 0$ [14, 28]. Consequently, the degree centrality of hyperedge e_i is given by

$$\mathcal{K}_i^e = \sum_{j=1}^M \mathcal{A}_{ij}, \quad (14)$$

Similarly to vector centrality, we evenly distribute the degree of the hyperedge of each hyperedge to the nodes associated with it. Given a node v_i that has an associated hyperedge set $E_i = \{e_{i1}, e_{i2}, \dots, e_{iK}\}$, the hyperedge degree centrality of v_i is

$$\mathcal{K}_i = \sum_{e_{ij} \in E_i} \frac{\mathcal{K}_{ij}^e}{|e_{ij}|}, \quad (15)$$

where \mathcal{K}_{ij}^e is the hyperedge degree centrality of e_{ij} .

Eccentricity centrality (ECC) is based on the hypothesis that highly influential hyperedges have a shorter distance from the other hyperedges.[1] Then, the eccentricity centrality of hyperedge e_i is defined as

$$\epsilon_i^e = \frac{1}{\max_{e_j \in C_1} \{d_1^e(i, j)\}}, \quad (16)$$

where C_1 represents the 1-connected component composed of 1-connected hyperedges. Similarly, we distribute the centrality value of the hyperedge evenly to each node within it. Given node v_i and its associated hyperedge set E_i , the eccentricity centrality of node v_i is given by the following equation:

$$\epsilon_i = \sum_{e_{ij} \in E_i} \frac{\epsilon_{ij}^e}{|e_{ij}|}, \quad (17)$$

where ϵ_{ij}^e is the eccentricity centrality of e_{ij} .

Harmonic closeness centrality (HCC) considers a hyperedge more critical if its average distance to other hyperedges is smaller[1]. The harmonic

closeness centrality score of a hyperedge is obtained by the following equation:

$$h_i^e = \frac{1}{M-1} \sum_{e_i, e_j \in E, i \neq j} \frac{1}{d_1^e(i, j)}, \quad (18)$$

The harmonic closeness centrality score is evenly distributed to each node associated with it, and the harmonic closeness centrality of a node v_i is defined as

$$h_i = \sum_{e_{ij} \in E_i} \frac{h_{ij}^e}{|e_{ij}|}, \quad (19)$$

where h_{ij}^e is the harmonic closeness centrality of e_{ij} .

4.2. Data description

We give a detailed description of the empirical hypergraphs, which are used to evaluate the proposed method for the characterization of node influence. Bars-Rev and Restaurants-Rev are hypergraphs of reviews collected from Yelp.com, where hyperedges consist of users who reviewed the same bar or restaurant. Music-Rev is a hypergraph of reviews collected from Amazon. Algebra and Geometry are collected from MathOverflow.net, with users who answered the same question forming hyperedges. Email-Enron describes emails sent between employees at Enron Corporation. The basic topological properties of these hypergraphs are presented in Table 1, where N represents the number of nodes, M is the number of hyperedges, $\langle k \rangle$ denotes the average degree, $\langle k^H \rangle$ represents the average hyperdegree, $\langle k^E \rangle$ is the average size of the hyperedges, $\langle l \rangle$ and C are the average shortest path length and average clustering coefficient of the corresponding simple networks, s_M denotes the maximum value of the adjacency relationship in the hypergraph, and β_0 represents the infection probability of the Monte Carlo simulation we use in the experiment.

Table 1: Basic topological properties of empirical hypergraphs.

Datasets	N	M	$\langle k \rangle$	$\langle k^H \rangle$	$\langle k^E \rangle$	$\langle l \rangle$	C	s_M	β_0
Bars-Rev	1234	1194	174.30	9.62	9.93	2.1	0.58	17	0.016
Restaurants-Rev	565	601	8.14	8.14	7.66	1.98	0.54	14	0.026
Music-Rev	1106	694	167.88	9.49	15.13	1.99	0.62	19	0.012
Algebra	423	1268	78.90	19.53	6.52	1.95	0.79	36	0.198
Geometry	580	1193	164.79	21.52	10.47	1.75	0.82	63	0.040
Email-Enron	143	1459	36.26	31.94	3.13	1.90	0.66	15	0.046

5. Experiments

To evaluate the performance of our proposed method and the baselines, we use the Kendall correlation coefficient τ ($\tau \in [-1, 1]$) as an evaluation metric, i.e., we compute the Kendall correlation between the node rankings of a specific centrality method and the ranking of the node influence by Monte Carlo simulation by setting each node as the seed. A higher value of τ means that the centrality method can better recognize influential nodes, and vice versa. In the SIR model, we use the recovery rate as $\mu = 0.1$, and the infection probability β_0 as shown in Table 1 is slightly higher than the spread threshold of each hypergraph. All the experiments are implemented in Python and executed independently on a server with a 2.20GHz Intel(R) Xeon(R) Silver 4114 CPU and 90GB of memory.

5.1. Parametric analysis

In HDF and EHDF, we have two parameters, namely r and s_m , that should be adjusted to better identify the influential nodes. In Figure 4 and 5, we display 3D heat maps to illustrate the impact of r ($r \in \{1, 2, 3, 4, 5\}$) and s_m ($1 \leq s_m \leq s_M$) on the performance of HDF and EHDF, respectively. As shown in the figure, the Kendall correlation coefficient decreases as r increases, indicating that we need to consider a large radius of the ball to better identify influential nodes. In the meantime, as s_m increases, the Kendall correlation coefficient initially rises and then remains roughly constant. Therefore, we choose $r = 1$ (except for Geometry for EHDF, where we choose $r = 2$) and $s_m = \frac{s_M}{2}$ as shown in Table 2 for HDF and EHDF in the following experiments.

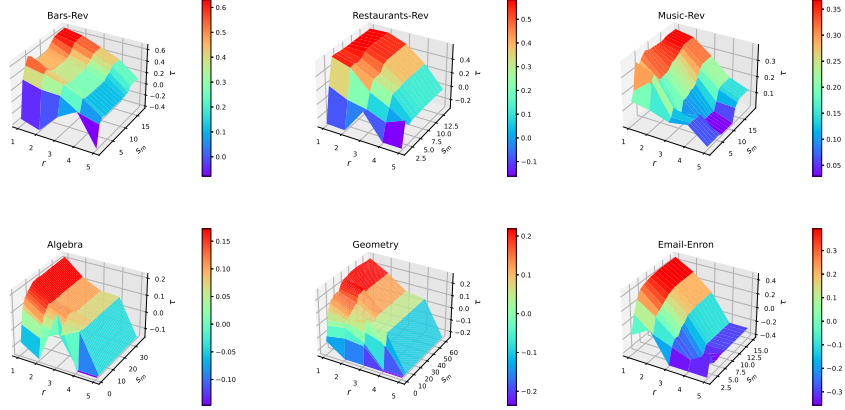


Figure 4: The change of parameters r and s_m on the performance of HDF in identifying influential nodes. We show the Kendall correlation coefficient for hypergraphs: Bars-Rev, Restaurants-Rev, Music-Rev, Algebra, Geometry and Email-Enron.

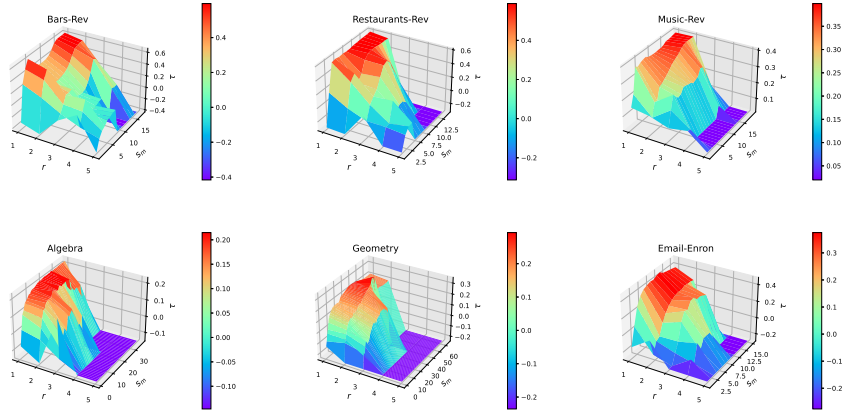


Figure 5: The change of parameters r and s_m on the performance of EHDF in identifying influential nodes. We show the Kendall correlation coefficient for hypergraphs: Bars-Rev, Restaurants-Rev, Music-Rev, Algebra, Geometry and Email-Enron.

Table 2: The optimal parameters r and s_m for the HDF and EHDF.

Hypergraph		Bars-Rev	Restaurants-Rev	Music-Rev	Algebra	Geometry	Email-Enron
HDF	s_m	15	3	7	26	34	10
	r	1	1	1	1	1	1
EHDF	s_m	4	13	19	24	40	10
	r	1	1	1	1	2	1

5.2. Performance of the proposed methods

We compare our method with the baselines to identify influential nodes, the results are given in Tables 3, 4 and Figure 6. In Table 3 and 4, we show the Kendall correlation coefficient τ between the node influence ranked by a particular centrality method and Monte Carlo simulation for $T = 100$ and $T = 500$. The highest values of τ are highlighted in bold and the second highest values are underlined for different empirical hypergraphs. The best performance is observed in HDF and EHDF on all hypergraphs for both $T = 100$ and $T = 500$, where our methods show even better performance for $T = 500$. Taking Table 3 as an example, EHDF outperforms in four hypergraphs, while HDF outperforms in two hypergraphs. The superiority of EHDF to HDF reveals that considering all the s -distances for the definition of radius can result in better identification of influential nodes. Beyond HDF and EHDF, DC also performs well in different hypergraphs. However, the rest of the baseline methods cannot identify influential nodes, some of them even showing negative values of τ . In reality, HDC acknowledges that nodes connected to more hyperedges are considered to have a higher degree of influence. However, the spreading model we have opted for randomly chooses a hyperedge for the contagion process. This implies that the actual influence of a node, based on its involvement in multiple hyperedges, does not necessarily hold true. Thus, the Kendall correlation coefficients for HDC and the actual spread capability of the nodes show a near-zero value in nearly all hypergraphs. VC, HEDC, ECC, and HCC are hyperedge-based techniques that evenly distribute hyperedge centrality scores to each node within the hyperedge in order to quantify the influence of the nodes. Nevertheless, as nodes within a hyperedge may have distinct roles, the equal distribution of hyperedge centrality scores may lead to an imprecise assessment of their influence. Additionally, the baselines such as ECC and HCC only consider lower-order distance between nodes, and show even worse performance than the other baseline methods. It should be noted that, as different values of T give similar results, we thus will use $T = 100$ in the following experiments.

Table 3 and 4 show the performance of the proposed methods in ranking

Table 3: The Kendall correlation coefficient τ between node influence ranked by a particular centrality method and Monte Carlo simulation. We show the results of six empirical hypergraphs: Bars-Rev, Restaurants-Rev, Music-Rev, Algebra, Geometry and Email-Enron. The best performance is shown in bold, and the second best is shown with an underline. We set $T = 100$.

Hypergraph	DC	HDC	VC	HEDC	ECC	HCC	HDF	EHDF
Bars-Rev	0.6236	0.0965	0.0680	-0.1783	-0.5725	-0.5490	0.6573	<u>0.6419</u>
Restaurants-Rev	0.5047	0.0469	0.0500	-0.0648	-0.4070	-0.3878	<u>0.5851</u>	0.5963
Music-Rev	0.0836	-0.2494	-0.2466	-0.2726	-0.4711	-0.4337	<u>0.3862</u>	0.3974
Algebra	<u>0.2525</u>	0.0362	0.03615	0.2115	-0.1671	-0.1276	0.2475	0.2556
Geometry	<u>0.2613</u>	-0.0495	-0.0504	-0.1644	-0.3056	-0.2998	0.2574	0.3368
Email-Enron	0.4376	-0.0920	-0.0937	-0.0580	-0.1372	-0.1110	0.4673	<u>0.4669</u>

Table 4: The Kendall correlation coefficient τ between node influence ranked by a particular centrality method and Monte Carlo simulation. We show the results of six empirical hypergraphs: Bars-Rev, Restaurants-Rev, Music-Rev, Algebra, Geometry and Email-Enron. The best performance is shown in bold, and the second best is shown with an underline. We set $T = 500$.

Hypergraph	DC	HDC	VC	HEDC	ECC	HCC	HDF	EHDF
Bars-Rev	0.6266	0.0915	0.0624	-0.1834	-0.5825	-0.5587	0.6623	<u>0.6541</u>
Restaurants-Rev	0.5077	0.0356	0.038	-0.0775	-0.4275	-0.4057	<u>0.6125</u>	0.6255
Music-Rev	0.0790	-0.2787	-0.2756	-0.3098	-0.5095	-0.472	<u>0.4076</u>	0.4137
Algebra	0.2361	-0.0163	-0.0164	-0.027	-0.2395	-0.1975	0.2550	<u>0.2612</u>
Geometry	<u>0.2657</u>	-0.0563	-0.0575	-0.1781	-0.3231	-0.3164	0.2626	0.3344
Email-Enron	<u>0.4727</u>	-0.0910	-0.0923	-0.0621	-0.1409	-0.1136	0.4809	0.4644

nodes globally. However, the top-ranked nodes are more important in reality. Therefore, we evaluate the centrality methods in identifying the top-ranked influential nodes in Figure 6, where the x-axis shows the top f fraction of nodes ($f \in \{5\%, 10\%, 15\%, 20\%, 25\%\}$) and the y-axis shows the overlap between the f fraction of the node sequence ranked by a specific centrality method and Monte Carlo simulation. The overlap O_{ij} between two sets B_i and B_j which have the same number of elements is defined as $O_{ij} = \frac{|B_i \cap B_j|}{|B_j|}$. The figures show that the top-ranked node sequences of EHDF and HDF are more overlapped with the SIR model-ranked node sequence across different hypergraphs and different fractions f of nodes, further implying that our method could better identify the influential top nodes than the baselines.

To gain a deeper understanding of the reasons behind the superior performance of the proposed methods compared to the baselines, we perform a more detailed analysis of the relationship between the centrality methods, and the results are given in Figures 7 to 12. For each hypergraph, we select the two best

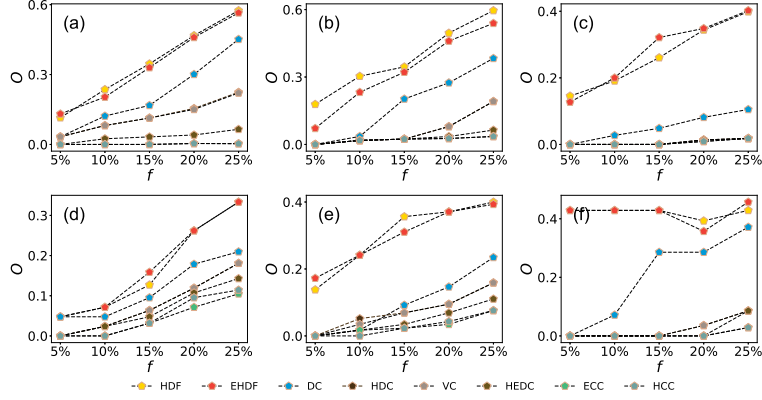


Figure 6: The overlap O between the top fraction of nodes (f) selected by centrality methods and the top fraction of nodes ranked by Monte Carlo simulation in hypergraphs: (a) Bars-Rev; (b) Restaurants-Rev; (c) Music-Rev; (d) Algebra; (e) Geometry and (f) Email-Enron.

and two worst performing methods evaluated by the Kendall correlation coefficient given in Tables 3 and 4, and show the correlation of each of these methods with HDF (Figures (a-d)) or EHDF (Figures (e-h)). Taking Bars-Rev as an example, DC and HDC perform the best apart from the methods we proposed, and ECC and HCC show the worst performance. In each of the figures, a point represents a node in the hypergraph, where the color of the points indicates the spreading capacity of the nodes (determined by Monte Carlo simulation), with the color transitioning from blue to yellow to indicate nodes with low to high influence. According to Figures 7 to 12, we observe a consistent pattern in all hypergraphs, i.e., the actual spreading ability of the nodes aligns closely with their centrality scores calculated using HDF (or EHDF). Specifically, blue nodes are predominantly located on the left side (corresponding to low HDF or EHDF values), while yellow nodes are predominantly located on the right side (corresponding to high HDF or EHDF values). However, the centrality values of the nodes in the baselines are not consistent with the real spread capacity of the nodes, which is in line with their bad performance illustrated in Tables 3, 4 and Figure 6. For example, nodes with degrees 50 to 800 share close values of spread ability in Bars-Rev. We further give the Pearson correlation coeffi-

cient (PCC) between the node sequence ranked HDF (EHDF) and the selected baselines, as shown in Figures 7 to 12. We observe that the proposed methods show high PCC values with the two best baselines and low PCC values with the worst ones.

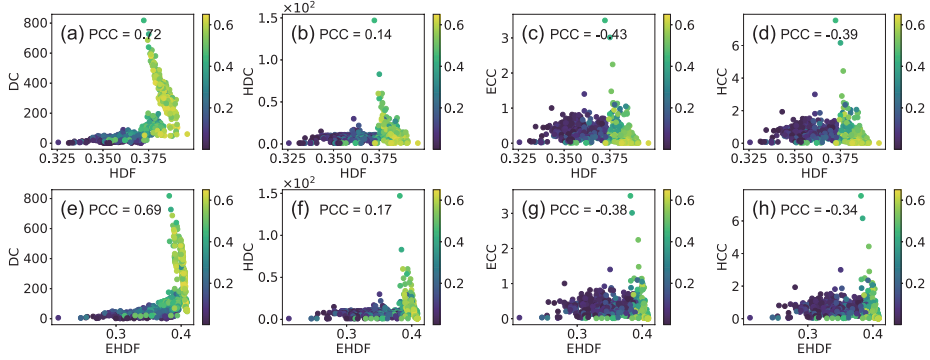


Figure 7: The correlation between the proposed methods (HDF and EDHF) and four baseline methods (DC, HDC, ECC, and HCC) in Bars-Rev. Each point in the figures shows a node in the hypergraph and the color of the points describes the spreading ability of the nodes. Figures (a-d) illustrate the correlation between HDF and four baselines. Figures (e-h) illustrate the correlation between EHDF and four baselines.

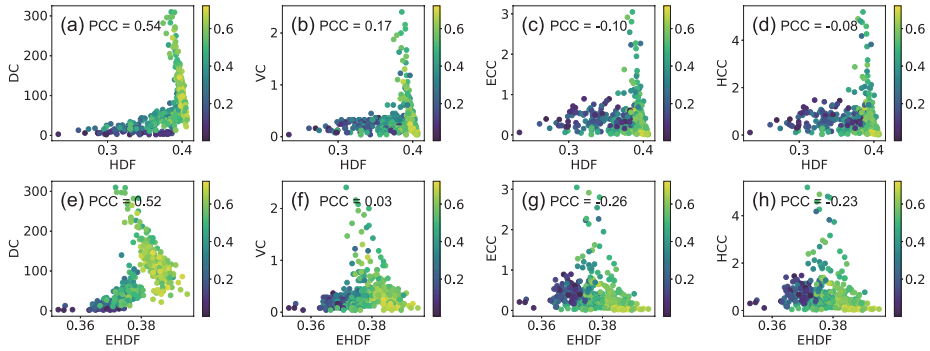


Figure 8: The correlation between the proposed methods (HDF and EDHF) and four baseline methods (DC, VC, ECC, and HCC) in Restaurants-Rev. Each point in the figures shows a node in the hypergraph and the color of the points describes the spreading ability of the nodes. Figures (a-d) illustrate the correlation between HDF and four baselines. Figures (e-h) illustrate the correlation between EHDF and four baselines.

To further evaluate the resilience of our approach, we conduct tests by modifying the infection probability $\beta = \gamma\beta_0$. The outcomes are presented in Figure 13. We calculate the Kendall correlation coefficient τ to examine the relation-

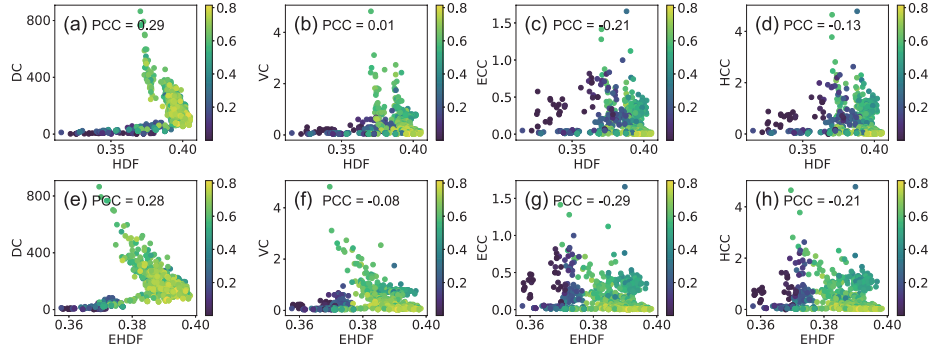


Figure 9: The correlation between the proposed methods (HDF and EDHF) and four baseline methods (DC, HDC, ECC, and HCC) in Music-Rev. Each point in the figures shows a node in the hypergraph and the color of the points describes the spreading ability of the nodes. Figures (a-d) illustrate the correlation between HDF and four baselines. Figures (e-h) illustrate the correlation between EDHF and four baselines.

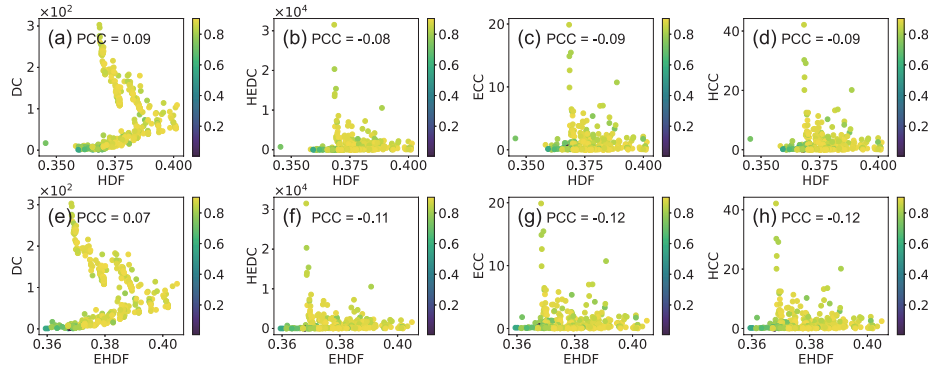


Figure 10: The correlation between the proposed methods (HDF and EDHF) and four baseline methods (DC, HEDC, ECC, and HCC) in Algebra. Each point in the figures shows a node in the hypergraph and the color of the points describes the spreading ability of the nodes. Figures (a-d) illustrate the correlation between HDF and four baselines. Figures (e-h) illustrate the correlation between EDHF and four baselines.

relationship between centrality scores obtained from various methods and the spread ability of nodes. The parameter γ ranges from 0.5 to 1.5, with an interval of 0.1. As the value of γ changes, HDF and EDHF consistently demonstrate stable and excellent performance. Similarly, the other baselines also maintain stable performance as γ varies, but show worse performance than our proposed methods. In particular, DC outperforms other baseline algorithms, especially in the Algebra network, where DC exhibits almost the best performance across different values of γ , yet HDF and EDHF remain highly competitive as well.

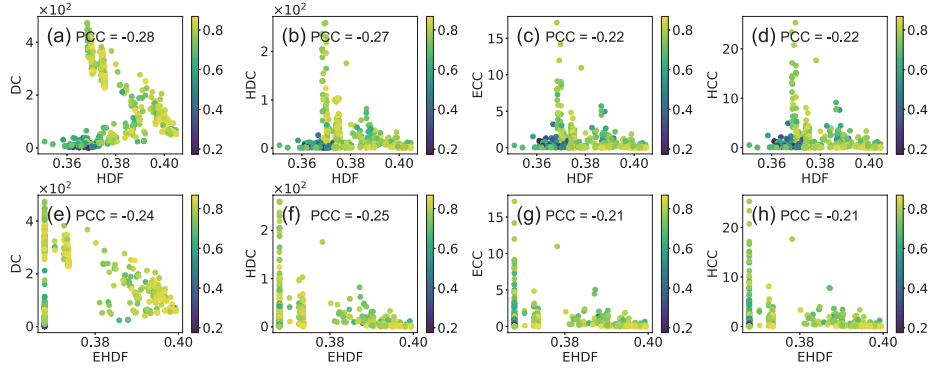


Figure 11: The correlation between the proposed methods (HDF and EDHF) and four baseline methods (DC, HDC, ECC, and HCC) in Geometry. Each point in the figures shows a node in the hypergraph and the color of the points describes the spreading ability of the nodes. Figures (a-d) illustrate the correlation between HDF and four baselines. Figures (e-h) illustrate the correlation between EDHF and four baselines.

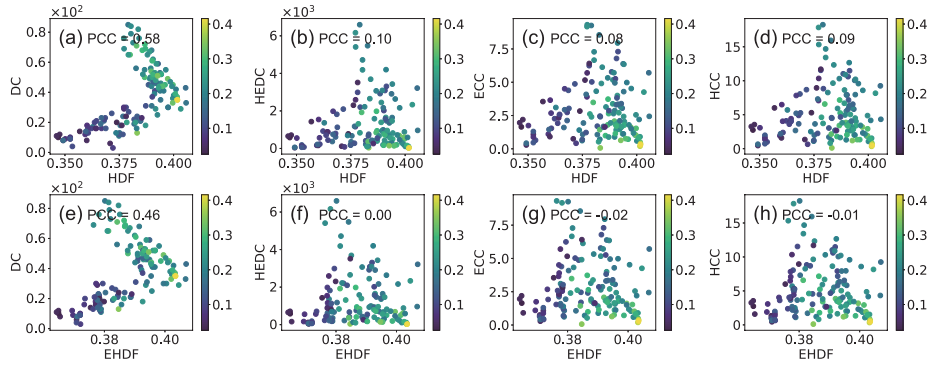


Figure 12: The correlation between the proposed methods (HDF and EDHF) and four baseline methods (DC, HeDC, ECC, and HCC) in Email-Enron. Each point in the figures shows a node in the hypergraph and the color of the points describes the spreading ability of the nodes. Figures (a-d) illustrate the correlation between HDF and four baselines. Figures (e-h) illustrate the correlation between EDHF and four baselines.

6. Discussion

6.1. Findings

In this study, we observe that the proposed approach, namely higher-order distance-based fuzzy centrality (HDF), shows outstanding effectiveness in the identification of influential nodes. The baselines are unable to accurately rank the influence of nodes or identify the most influential nodes due to their limitations, such as only considering local or low-order information of a hypergraph.

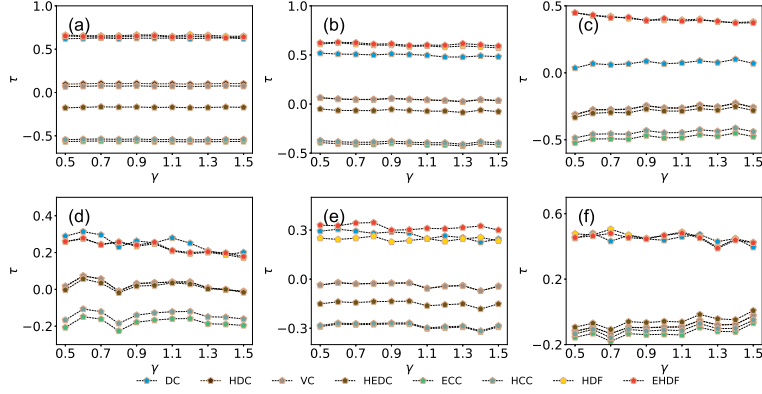


Figure 13: Kendall correlation coefficient τ between centrality scores obtained from various methods and the spread ability of nodes at various parameter γ in the six empirical hypergraphs: Bars-Rev, Restaurants-Rev, Music-Rev, Algebra, Geometry and Email-Enron.

In contrast, the experimental results suggest that HDF and EHDF, which incorporate higher-order information, could identify influential nodes with high accuracy.

6.2. Theoretical contribution

This study sheds light on the problem of locating influential nodes on hypergraphs and addresses the inadequacies in previous research regarding the utilization of higher-order information. In the design of higher-order distance-based fuzzy centrality, the influence of a target node is dependent on the influence of neighboring nodes at different higher-order distances, and the influence is collected by a nonlinear function that incorporates fuzzy sets and Shannon entropy. The effectiveness of our approach is dependent on the utilization of an adjustable radius for the ball in order to ascertain the neighboring nodes of each target node, as well as the non-linear function. This offers a theoretical support for identifying influential nodes in higher-order networks.

6.3. Practical significance

The investigation of identifying high-influence nodes on hypergraphs is of great practical importance, as many real-world systems involve complex inter-

actions among entities, represented by hyperedges. This research expands the potential applications of high-influence node identification to various domains, including viral marketing, epidemic prevention, and social opinion management.

7. Conclusion

The spreading dynamics on a hypergraph is usually not only through pairwise interactions, but also through higher-order interactions involving multiple nodes. In this work, we tackle the problem of identifying influential nodes in a hypergraph that could characterize higher-order interactions between nodes. We start with the definition of higher-order distance and describe the SIR spreading model, which aims to model the real influence of a node in a hypergraph. Based on the fuzzy collective influence that collects the influence of nodes inside the ball using fuzzy sets and Shannon entropy to quantify the influence of the target node, we propose a higher-order distance-based fuzzy centrality (i.e., HDF and EHDF) to solve the problem. To validate the effectiveness of our methods, we perform experiments on six empirical hypergraphs from various domains. The results show that our methods are superior to state-of-the-art benchmarks in terms of ranking influential nodes, especially in identifying the top influential nodes.

Despite the effectiveness of HDF and EHDF in identifying influential nodes, the proposed methods utilize a high-order distance between nodes, which is with high computational complexity, especially for large-scale networks. Therefore, one possible direction for future work could focus on proposing approaches to efficiently calculate the higher-order distance. Besides, the theoretical framework we have proposed for the identification of influential nodes has the potential to be applied to other types of higher-order networks, including simplicial complexes [24], temporal hypergraphs [7], and multilayer hypergraphs [36].

8. CRediT authorship contribution statement

Su-Su Zhang: Conceptualization, Methodology, Formal Analysis, Investigation, Original Draft Preparation, Review & editing. **Xiaoyan Yu:** Investigation, Original Draft Preparation, Data Curation, Visualization. **Chuang Liu:** Conceptualization, Methodology, Supervision, Review & editing. **Xiu-Xiu Zhan:** Conceptualization, Methodology, Validation, Investigation, Supervision, Review & editing.

9. Data and code availability

Data will be available on request.

10. Acknowledgments

This work was supported by the Natural Science Foundation of Zhejiang Province (Grant No. LQ22F030008), the Natural Science Foundation of China (Grant No. 61873080) and the Scientific Research Foundation for Scholars of HZNU (2021QDL030).

References

- [1] Aksoy, S.G., Joslyn, C., Marrero, C.O., Praggastis, B., Purvine, E., 2020. Hypernetwork science via high-order hypergraph walks. *EPJ Data Science* 9, 1–34.
- [2] Albert, R., Barabási, A.L., 2002. Statistical mechanics of complex networks. *Reviews of Modern Physics* 74, 47–97.
- [3] Alkhodair, S.A., Ding, S.H., Fung, B.C., Liu, J., 2020. Detecting breaking news rumors of emerging topics in social media. *Information Processing & Management* 57, 102018.
- [4] Berge, C., 1985. *Graphs and hypergraphs*. Elsevier Science Ltd.

- [5] Bian, T., Hu, J., Deng, Y., 2017. Identifying influential nodes in complex networks based on ahp. *Physica A: Statistical Mechanics and its Applications* 479, 422–436.
- [6] Boccaletti, S., Latora, V., Moreno, Y., Chavez, M., Hwang, D.U., 2006. Complex networks: Structure and dynamics. *Physics Reports* 424, 175–308.
- [7] Cencetti, G., Battiston, F., Lepri, B., Karsai, M., 2021. Temporal properties of higher-order interactions in social networks. *Scientific Reports* 11, 1–10.
- [8] Chen, D.B., Xiao, R., Zeng, A., Zhang, Y.C., 2014. Path diversity improves the identification of influential spreaders. *Europhysics Letters* 104, 1–6.
- [9] Cimini, G., Squartini, T., Saracco, F., Garlaschelli, D., Gabrielli, A., Caldarelli, G., 2019. The statistical physics of real-world networks. *Nature Reviews Physics* 1, 58–71.
- [10] Curado, M., Tortosa, L., Vicent, J.F., 2023. A novel measure to identify influential nodes: return random walk gravity centrality. *Information Sciences* 628, 177–195.
- [11] Guo, W.F., Zhang, S.W., Shi, Q.Q., Zhang, C.M., Zeng, T., Chen, L., 2018. A novel algorithm for finding optimal driver nodes to target control complex networks and its applications for drug targets identification. *Bmc Genomics* 19, 67–79.
- [12] Gupta, M., Mishra, R., 2021. Spreading the information in complex networks: Identifying a set of top-n influential nodes using network structure. *Decision Support Systems* 149, 113608.
- [13] Harrold, J., Ramanathan, M., Mager, D., 2013. Network-based approaches in drug discovery and early development. *Clinical Pharmacology & Therapeutics* 94, 651–658.

- [14] Hu, F., Ma, L., Zhan, X.X., Zhou, Y., Liu, C., Zhao, H., Zhang, Z.K., 2021. The aging effect in evolving scientific citation networks. *Scientometrics* 126, 4297–4309.
- [15] Jiang, J., Wen, S., Yu, S., Xiang, Y., Zhou, W., 2016. Identifying propagation sources in networks: State-of-the-art and comparative studies. *IEEE Communications Surveys & Tutorials* 19, 465–481.
- [16] Jiang, Z.Y., Zeng, Y., Liu, Z.H., Ma, J.F., 2019. Identifying critical nodes' group in complex networks. *Physica A: Statistical Mechanics and its Applications* 514, 121–132.
- [17] Kovalenko, K., Romance, M., Vasilyeva, E., Aleja, D., Criado, R., Musatov, D., Raigorodskii, A.M., Flores, J., Samoylenko, I., Alfaro-Bittner, K., et al., 2022. Vector centrality in hypergraphs. *Chaos, Solitons & Fractals* 162, 112397.
- [18] Li, F., Xu, H., Wei, L., Wang, D., 2023. Identifying vital nodes in hyper-network based on local centrality. *Journal of Combinatorial Optimization* 45, 32.
- [19] Liu, X., Zhao, C., 2023. Eigenvector centrality in simplicial complexes of hypergraphs. *Chaos: An Interdisciplinary Journal of Nonlinear Science* 33, 093109.
- [20] Liu, Y., Jin, X., Shen, H., 2019. Towards early identification of online rumors based on long short-term memory networks. *Information Processing & Management* 56, 1457–1467.
- [21] Liu, Y., Wang, J., He, H., Huang, G., Shi, W., 2021. Identifying important nodes affecting network security in complex networks. *International Journal of Distributed Sensor Networks* 17, 1–10.
- [22] Lü, L., Chen, D., Ren, X.L., Zhang, Q.M., Zhang, Y.C., Zhou, T., 2016. Vital nodes identification in complex networks. *Physics Reports* 650, 1–63.

- [23] Parand, F.A., Rahimi, H., Gorzin, M., 2016. Combining fuzzy logic and eigenvector centrality measure in social network analysis. *Physica A: Statistical Mechanics and its Applications* 459, 24–31.
- [24] Raj, U., Bhattacharya, S., 2023. Some generalized centralities in higher-order networks represented by simplicial complexes. *Journal of Complex Networks* 11, 1–25.
- [25] Shannon, C.E., 1948. A mathematical theory of communication. *The Bell system technical journal* 27, 379–423.
- [26] Stegehuis, C., Peron, T., 2021. Network processes on clique-networks with high average degree: the limited effect of higher-order structure. *Journal of Physics: Complexity* 2, 045011.
- [27] Tudisco, F., Higham, D.J., 2021. Node and edge nonlinear eigenvector centrality for hypergraphs. *Communications Physics* 4, 1–10.
- [28] Wang, J.W., Rong, L.L., Deng, Q.H., Zhang, J.Y., 2010. Evolving hyper-network model. *The European Physical Journal B* 77, 493–498.
- [29] Wang, X., Slamu, W., Guo, W., Wang, S., Ren, Y., 2022a. A novel semi local measure of identifying influential nodes in complex networks. *Chaos, Solitons & Fractals* 158, 112037.
- [30] Wang, Y., Li, H., Zhang, L., Zhao, L., Li, W., 2022b. Identifying influential nodes in social networks: Centripetal centrality and seed exclusion approach. *Chaos, Solitons & Fractals* 162, 112513.
- [31] Xie, M., Zhan, X.X., Liu, C., Zhang, Z.K., 2023a. An efficient adaptive degree-based heuristic algorithm for influence maximization in hypergraphs. *Information Processing & Management* 60, 103161.
- [32] Xie, X., Zhan, X., Zhang, Z., Liu, C., 2023b. Vital node identification in hypergraphs via gravity model. *Chaos: An Interdisciplinary Journal of Nonlinear Science* 33, 013104.

- [33] Young, J.G., Petri, G., Peixoto, T.P., 2021. Hypergraph reconstruction from network data. *Communications Physics* 4, 135.
- [34] Zadeh, L.A., 1997. Toward a theory of fuzzy information granulation and its centrality in human reasoning and fuzzy logic. *Fuzzy sets and systems* 90, 111–127.
- [35] Zhang, Q., Shuai, B., Lü, M., 2022. A novel method to identify influential nodes in complex networks based on gravity centrality. *Information Sciences* 618, 98–117.
- [36] Zhen, Y., Wang, J., 2023. Community detection in general hypergraph via graph embedding. *Journal of the American Statistical Association* 118, 1620–1629.